DOI: 10.23968/2500-0055-2023-8-4-47-56

## EVALUATION OF BASALT FIBER REINFORCED ROLLER COMPACTED CONCRETE CONTAINING COAL POWDER FOR PAVEMENT

Sadik Alper Yildizel*, Kemal Armagan

Karamanoğlu Mehmetbey University, Engineering Faculty, Karaman, Türkiye

*Corresponding author's e-mail: sayildizel@kmu.edu.tr

**Abstract**
**Introduction**: The utilization of colored roller compacted concrete (RCC) for pavements in order to mitigate the urban heat island effect is a popular approach: increasing solar reflectance can reduce the effect. The paper explores the possibility of applying the reverse mechanism for regions with cold climates. The **purpose of the study** was to evaluate the mechanical, durability and solar reflectance properties of roller compacted concrete with coal powder (CP) and basalt fiber (BF) additives for pavement. **Methods:** an UV-Vis-NIR spectrophotometer was utilized for the albedo measurements. Consistency of the specimens was determined with Vebe consistometer. Compressive, flexural, and splitting tensile strengths were recorded at 7, 28 and 90 days. Frost resistance of the specimens was also investigated. **Result:** The combined utilization of 5% CP and 0.5% BF showed great performance for the roller compacted concrete pavements. Furthermore, the obtained albedo values also have the potential to increase the ambient temperature in cold climates.

**Keywords:** coal powder, basalt fiber, albedo, concrete, roller compacted concrete.

### Introduction

One of the most widely used forms of carbon is coal, which was produced in the United States alone to the tune of 756.2 million tons in 2018 (Masi et al., 2021). In addition to being used for the production of thermal energy, city heating, and coal chemical conversion (Ren et al., 2022), coal currently meets 41% of the world's electricity needs (Xu et al., 2022). Along with providing heat for the wallboard, aluminum, and cement industries, significant amounts of coal are also used in metallurgical processes, gasification, the cement industry, and as a source of activated carbon and many other common and industrial chemicals (Dai and Finkelman, 2018).

Basalt fibers (BF) are renowned for their ability to absorb energy, to bond with the matrix, to resist mechanical and chemical properties, and to exhibit significant acoustic and thermal characteristics (Vinotha Jenifer et al., 2023). Compared to glass fibers, basalt fiber has a better tensile strength and is more affordable. In terms of resistance to fire, chemical attack, sudden load, and good strain capacity, basalt fiber outperforms carbon fiber (Meesaraganda et al., 2023). To create basalt fiber-reinforced concrete (BFRC), BF can be incorporated into concrete as chopped fibers. The impact of using BF in BFRC on compressive strength varies across studies. With a specific dosage of BF, the compressive strength increased in some studies, decreased or did not show any significant effect in others (Al-Rousan et al., 2023).

Compared to other naturally occurring surfaces like vegetation and the earth, man-made or built-up surfaces like concrete and asphalt absorb more heat from sunlight. The urban heat island (UHI) effect is caused by the air being heated by the heat stored in the pavements. Because it is light gray instead of black, concrete has a much higher initial albedo than asphalt. However, over time, due to weathering and the buildup of dirt, the albedo of concrete decreases. Albedo's typical starting value for fresh concrete is 0.35 to 0.40, and for weathered concrete it is 0.25 to 0.30 (Reza and Boriboonsomsin, 2015).

Concrete materials have high thermal inertia and they are gray in color. They absorb a lot of solar radiation and then release it into the air as sensible heat, which helps create urban heat islands. The solar reflectance of building walls, roofs, and streets — the large proportion of which are made of hardened Portland cement concrete — determines the intensity of urban heat islands. Increasing the solar reflectance, or albedo, of building and street surfaces would reduce the urban heat island effect by decreasing heat convection from these surfaces to the air (Qin et al., 2019).

Roller compacted concrete (RCC) is a zero-slump concrete that is made of sand, Portland cement, dense-graded aggregate, and water. It is typically laid out using an asphalt paver and compacted using regular vibratory roller compactors (Modarres and Hosseini, 2014). Compared to traditional concrete, RCC contains more aggregate, less cement, and less water. To increase its densification, compaction energy must be applied (Lam et al., 2017; Meddah et al., 2014). To achieve the desired density and homogeneous surface pavement, it is placed using a standard or high-density asphalt-type paver equipment and compacted by vibratory rollers. When compared to conventional rigid pavement or asphaltic pavement, RCC can reduce the cost of pavement construction by 15% to 30% while also allowing for an earlier opening to traffic (LaHucik et al., 2017; Mohammed and Adamu, 2018).

This study explores the mechanical and durability behaviors of RCC with basalt fiber and coal powder additives. The objective was to obtain better albedo results in RCC with these additives. The main purpose of this study was to determine: (1) the mechanical properties of RCC with basalt fiber and coal powder additives; (2) the durability properties of RCC with basalt fiber and coal powder additives; (3) the effect of adding coal powder in RCC to albedo characteristic. The results of this study can provide a possibility of replacing lower albedo traditional concrete with coal powder RCC to increase UHI in urban areas.

**Methods**

In the experimental study, crushed limestone and silica sand (SS) were used as coarse aggregate (CA) and fine aggregate (FA), respectively. Organic content of the aggregates was removed after the air-drying process. Maximum aggregate size was selected as 20 mm for preventing any possible segregation and its effects. Combined gradation curves of the aggregates are presented in Fig. 1. CEM II type (42.5R) white cement (WC) conforming to BS EN 197(British Standard Institution BSI, 2011) standard was also used. Commercially available coal powder (CP) was utilized as filler and cement replacement material. Cement replaced with CP at the ratios of 5%, 10%, 15% and 20% by the weight of cement. Chemical compositions of the CP and WC are given in Table 1. Basalt fibers (BF: 8 mm length) were utilized with the ratios of 0.25%, 0.5%, 0.75%, and 1% by volume of the mixtures. Water-to-cement ratios were selected between 0.40 and 0.44 in order to meet the requirements of ACI 207.R-11 (ACI, 2011) regarding permissible compaction and water content limits. Utilized CP, BF and WC are given in Fig. 2. According to the ASTM C1435 standard, a compactor was used to compact the mixtures in three layers at blow counts of 1000 and 1850 r/min (10 kg of surcharge). The optimal water content values of the prepared mixtures were well within the limits.

Albedo values of the specimens were measured with an UV-Vis-NIR spectrophotometer (Fig. 3). 24 mm x 24 mm x 5 mm rectangular specimens were prepared for this measurement (Fig. 4). Wavelengths between 200–2500 nm were investigated to determine albedo properties. Mean reflection percentages were measured and albedo values of each specimen were determined according to the measurement of the spectrophotometer.

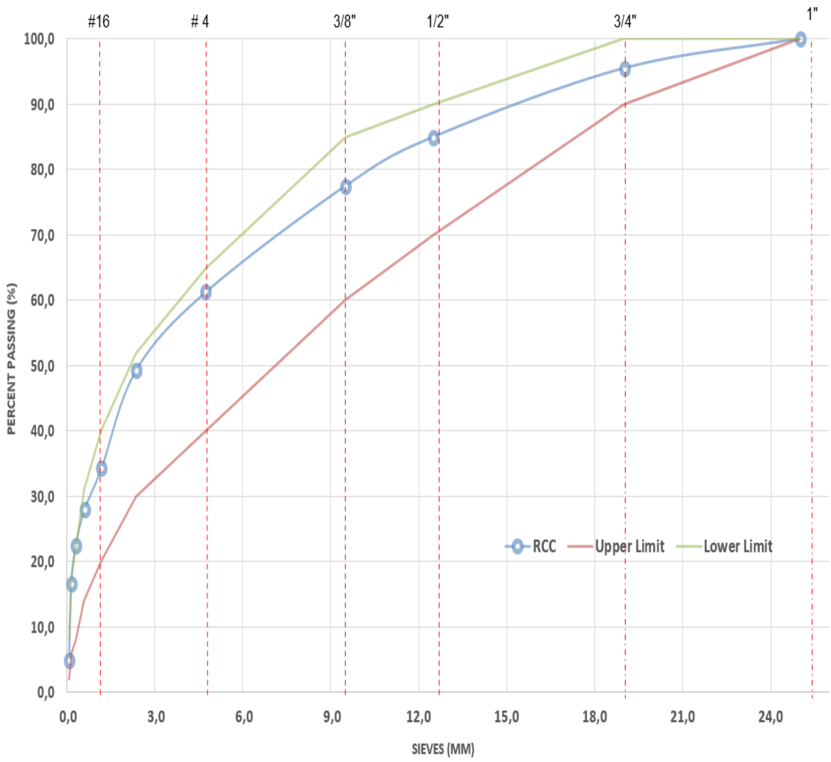


Fig. 1. Combined aggregate gradation curves

The mixtures were blended using a pan mixer (60 L) with a constant rate of 250 r/min. The consistency of all mixtures was recorded with a Vebe test device according to the ASTM C1170 (ASTM, 2014) standard. Compressive strength tests and splitting tensile tests were conducted on the 150 mm x 300 mm cylindrical specimens as per the guidance of ASTM C39 (ASTM, 2016), ASTM C496 (ASTM, 2011) for 7, 28 and 90 days, respectively. 100 mm x 100 mm x 500 mm rectangular specimens were prepared for the flexural strength test. And the loading rate kept constant at 0.9 MPa/min in accordance with ASTM C39 (ASTM, 2016). Frost resistance of the specimens (100 cycles) was also determined as per ASTM C666 (Morgan, 1991).

The albedo values of the specimens were measured at the first step during the experimental studies after 28 days of curing. Each specimen's spectral reflectance was measured three times. The mean of the three measurements was recorded. Afterwards, mechanical and durability tests were carried out. The mix design proportions and flow chart of the experimental studies are given in Table 2 and Fig. 5, respectively.

Table 1. **Chemical ingredients of WC and CP** (provided by the supplier)

| Component (%) | WC | CP |
|---|---|---|
| $Fe_2O_3$ | 3.5 | 3.82 |
| CaO | 60.48 | 0.49 |
| $Al_2O_3$ | 4.32 | 14.47 |
| MgO | 2.37 | 0.85 |
| $SiO_2$ | - | 33.9 |
| Free CaO | 1.69 | - |
| $SO_3$ | 2.61 | - |
| $Na_2O$ | - | 0.25 |
| $K_2O$ | - | 2.32 |
| MnO | - | 0.02 |
| $TiO_2$ | - | 0.941 |

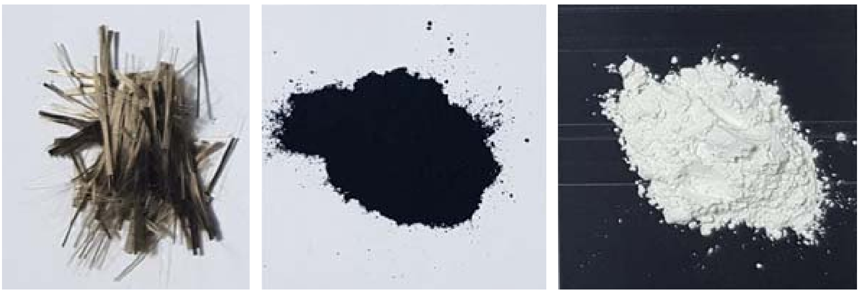

Basalt Fiber | Coal Powder | White Cement (42.5 R)

Fig. 2. Basalt fiber, coal powder and white cement

**Results and discussion**

The calculated albedo values of the prepared specimens are presented in Fig. 6. Test results vary between 0.28 and 0.16. Reference mixture with no CP and BF content showed the highest albedo of 0.28, as expected (Kaloush et al., 2008). This lowest result can be attributed to ingredients of the reference mixture since the albedo of concrete is generally correlated with the albedo of cement and aggregates (Levinson and Akbari, 2002). Albedo decreased with the increasing CP content (Emery et al., 2014). Albedo of the concrete specimens increased with the increasing water-to-cement ratios (Qin et al., 2019) due to the more possible formation of $Ca(OH)_2$ as a hydration product (Chaussadent et al., 2000). However, this phenomenon is not valid for color-incorporated concrete according to the albedo test results.

Vebe test results are presented in Fig. 7. The test results showed that Vebe time increased with the


Fig. 3. UV-Vis-NIR spectrophotometer

Fig. 4. CP added specimens

Table 2. **Mixture proportions**

| Mixture code | WC (kg/m³) | CP (kg/m³) | BF (%) | FA (kg/m³) | CA (kg/m³) | W/C | Optimum water content (%) |
|---|---|---|---|---|---|---|---|
| R | 270 | - | - | 750 | 1130 | 0.41 | 5.31 |
| $P_1$ | 256.5 | 13.5 | 0.25 | 750 | 1130 | 0.42 | 5.45 |
| $P_2$ | 243 | 27 | 0.5 | 750 | 1130 | 0.43 | 5.92 |
| $P_3$ | 229.5 | 40.5 | 0.75 | 750 | 1130 | 0.44 | 6.27 |
| $P_4$ | 216 | 54 | 1 | 750 | 1130 | 0.45 | 6.43 |

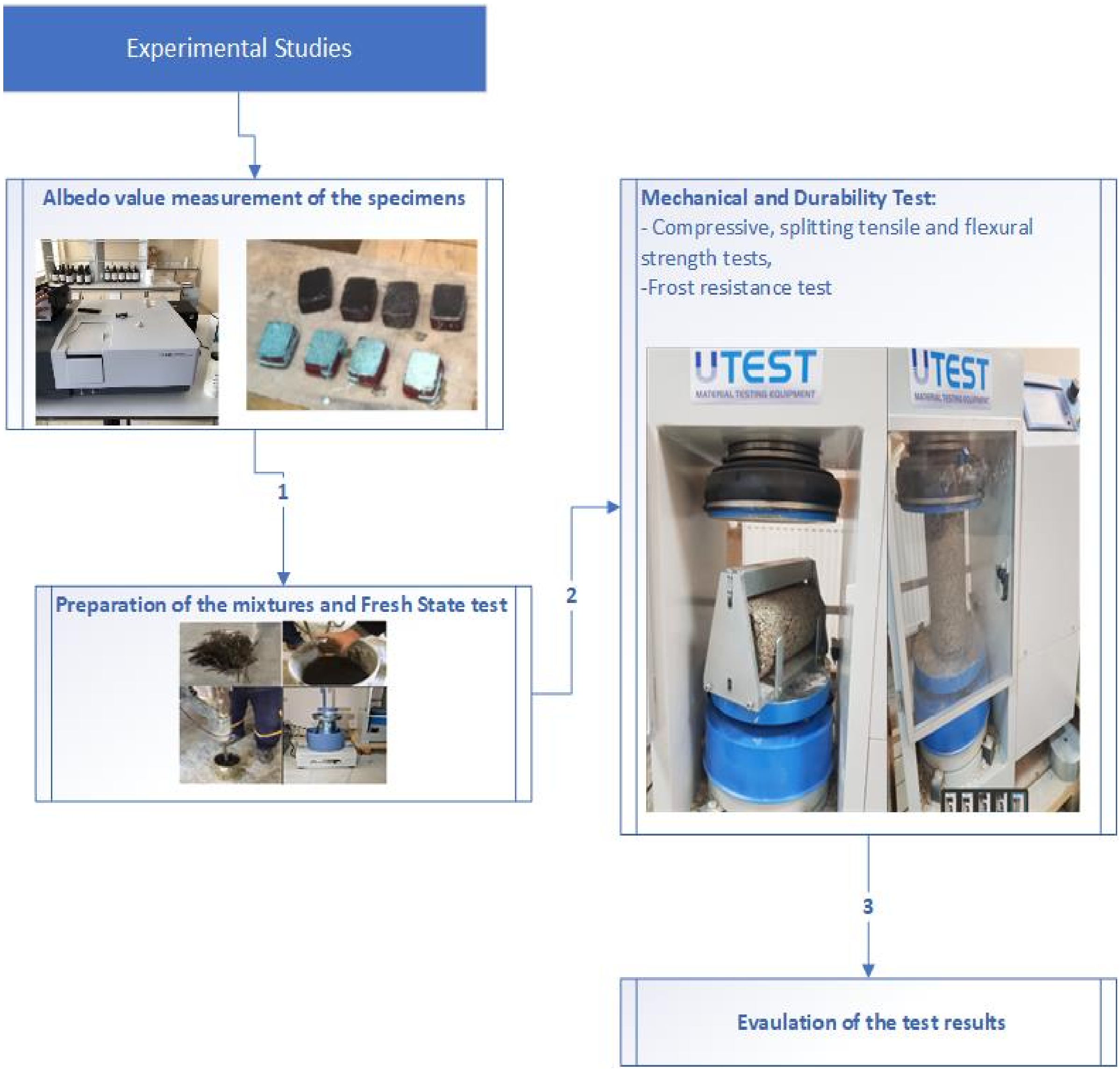


Fig. 5. Flow chart of the experimental studies

increasing CP replacement levels and BF contents. The Vebe time was 48 s for the control mix, and 69 s for the $P_4$ specimen. For such mixtures, this increase was related to the higher water absorption rate of coal powder (Argiz et al., 2018; Singh et al., 2020) and increased BF content that holds the mixture and slow aggregate settlement (Kirthika and Singh, 2018).

Compressive strength test results are presented in Fig. 8. The reported compressive strength values were calculated by the mean of the three specimens. Except $P_4$, all specimens met the requirements of ACI 325 (ACI, 2001) (min. 27.6 MPa for 28-day strength). The use of 5% CP together with the 0.25% BF was found to increase the compressive strength by 10.1% and outperformed other mixtures. The results also

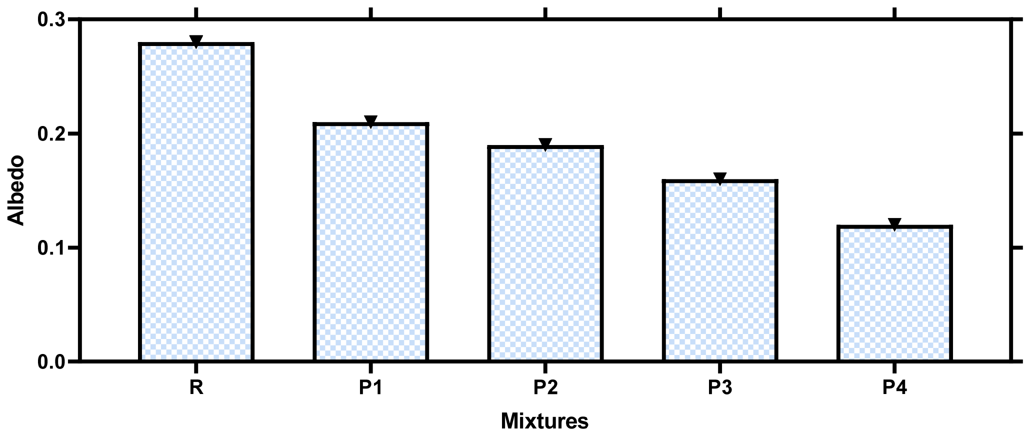


Fig. 6. Albedo values of the specimens

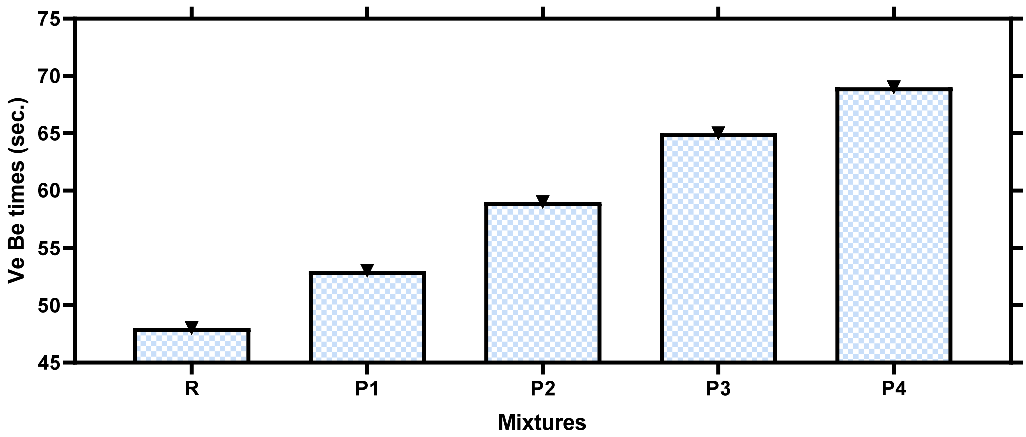


Fig. 7. Consistency of the mixtures

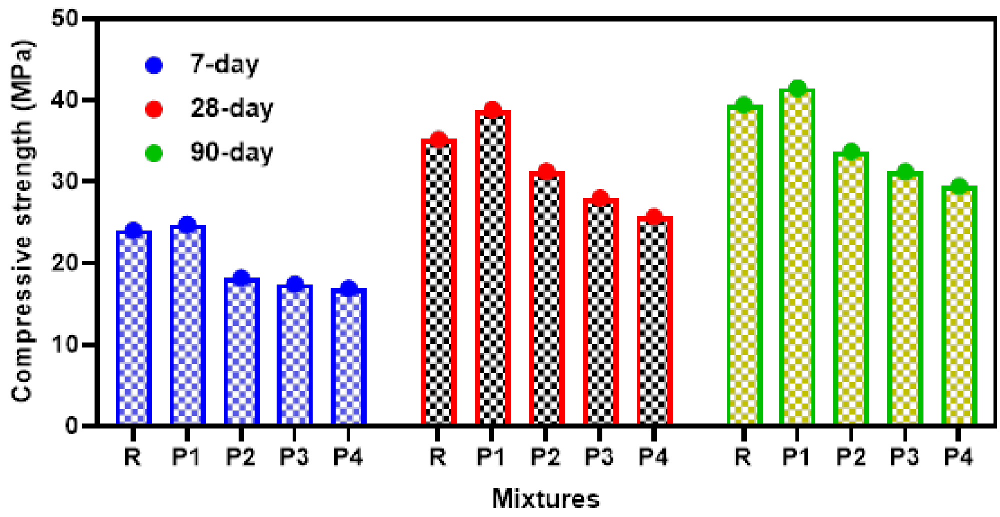


Fig. 8. Compressive strength test results

showed that increasing the CP replacement level by more than 5% reduced the compressive strength (Hesami et al., 2016). The compressive strength was reduced by approximately 50% by utilizing 20% CP and 1% BF at 28 days. This reduction is attributed to the low cement (Radović et al., 2021) and high BF contents of $P_4$. Higher amount of BF (Liang et al., 2021) could lead to poorer interfaces between fibers and cement matrix (Algin and Ozen, 2018).

Fig. 9 shows the flexural strength test results. According to Fig. 8, the recorded flexural strength varied in the range of 3.1 and 5.34 MPa. The combined utilization of 0.5% BF and 10% CP enhanced the flexural test results up to 20% compared to the reference mixtures at 28 days. These results also agree with the earlier studies (Haido et al., 2021; Hesami et al., 2016; Liang et al., 2021; Modarres et al., 2018), which showed that the CP replacement level of more than 10% and the BF exceeding 0.5% in volume fraction reduced the flexural strength. The flexural to compressive strength ratios at 28 days varied within the range of 14.85 and 23.1 MPa. This finding was also reported in the paper by Hesami et al. (2016), which stated that the ratios were calculated as higher values compared to the traditional concrete.

Splitting tensile strength test results are given in Fig. 10. The results show that the splitting tensile strength varied between 2.41 and 3.84 MPa. The splitting tensile to compressive strength ratios of this study were calculated within the range of 6.8% and 11.9%, which are consistent with data obtained in earlier studies (Choi and Yuan, 2005; Gaedicke, 2016). Another finding is that the splitting tensile strength decreased by increasing CP and BF content by more than 5% and 0.5%, respectively.

Compressive strength losses after 100 freezing & thawing cycles at 90 days are given in Fig. 11. The compressive strength losses of this research were measured between 4.2% and 26.7%. $P_4$ specimen performed the worst with 26.7 % strength loss. This can be attributed to the excessive BF and CP content, which hindered the connections of the cementitious materials (Yuan et al., 2020). $P_1$ showed the best performance with 5% CP and 0.5% BF content. The order of the specimens from strong to weak was obtained as $P_1 > R > P_2 > P_3 > P_4$.

**Conclusion**

In this study, coal powder added roller compacted concrete reinforced with basalt fiber was evaluated in terms of its solar reflectance, mechanical and durability properties. The combined effect of basalt fiber and coal powder was investigated as well. The main conclusion of the study can be drawn as follows:

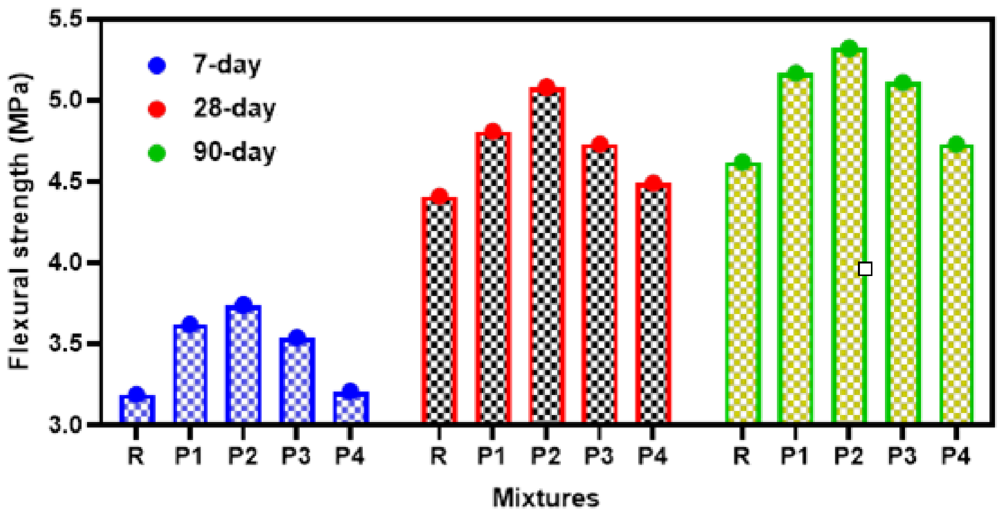


Fig. 9. Flexural strength test results

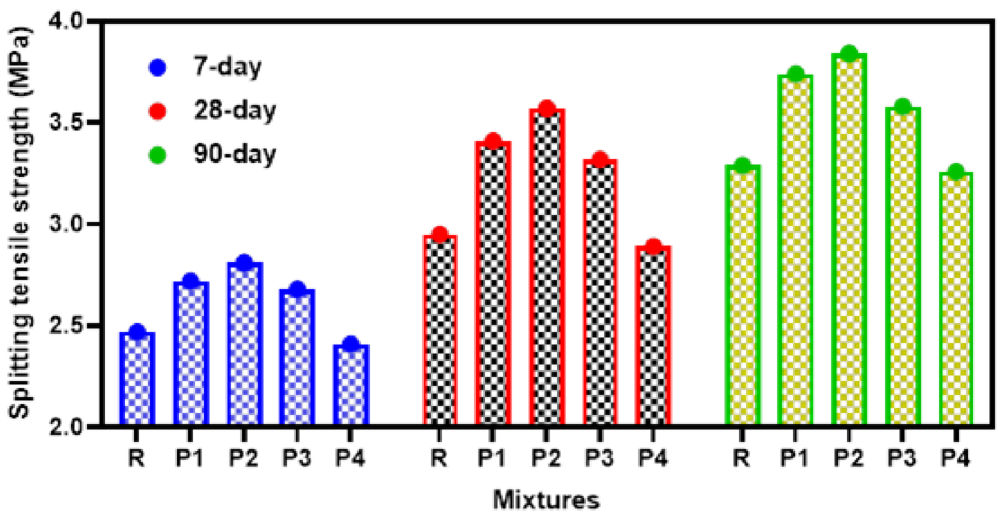


Fig. 10. Splitting tensile strength test results

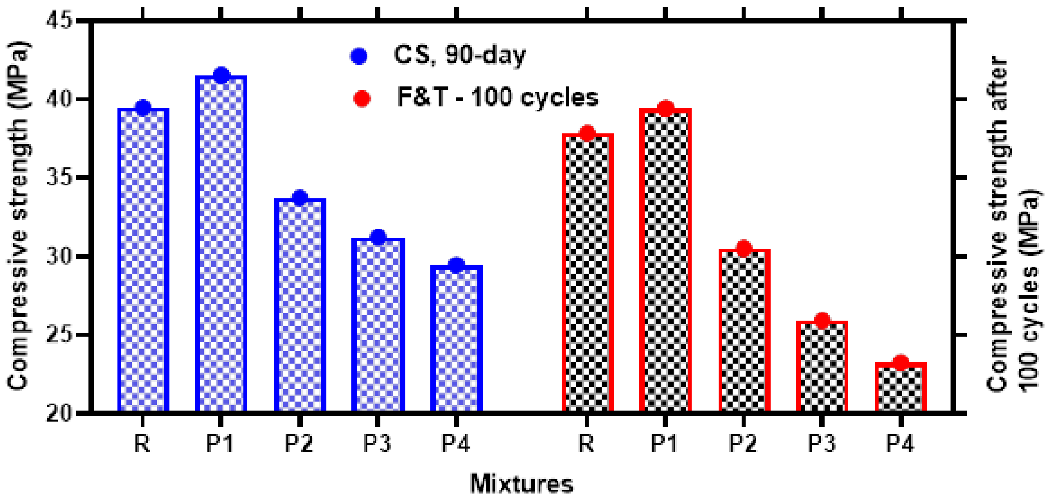


Fig. 11. Compressive strength losses after 100 cycles

- Basalt fiber additives and the partial replacement of cement by coal powder produce higher optimum moisture content, Vebe times and water-to-cement ratio.
- The combination of 5% CP and 0.5% BF enhanced the mechanical properties of the roller concrete specimens.
- The potential replacement of CP in roller compacted concrete production was also investigated and the utilization of CP as cement supplementary material up to 5% can lead to a greener concrete design.
- Inclusion of 5% CP and 0.5% BF improved the frost resistance of concrete specimens after 100 cycles.
- According to the albedo within the scope of the study, future concretes can be designed to reduce or increase the urban heat island effect.

**References**


ACI (2001). ACI 325.11R-01. Accelerated techniques for concrete paving. Reported by ACI Committee 325. Farmington Hills: American Concrete Institute, USA, pp. 8-11.

ACI (2011). *ACI 207.5R-11. Report on rolller-compacted mass concrete*. Farmington Hills: American Concrete Institute, USA, pp. 6-7.

Algin, Z. and Ozen, M. (2018). The properties of chopped basalt fibre reinforced self-compacting concrete. *Construction and Building Materials*, Vol. 186, pp. 678–685. DOI: 10.1016/j.conbuildmat.2018.07.089.

Al-Rousan, E. T., Khalid, H. R., and Rahman, M. K. (2023). Fresh, mechanical, and durability properties of basalt fiber-reinforced concrete (BFRC): A review. *Developments in the Built Environment*, Vol. 14, 100155. DOI: 10.1016/j.dibe.2023.100155.

Argiz, C., Moragues, A., and Menéndez, E. (2018). Use of ground coal bottom ash as cement constituent in concretes exposed to chloride environments. *Journal of Cleaner Production*, Vol. 170, pp. 25–33. DOI: 10.1016/j.jclepro.2017.09.117.

ASTM (2011). *ASTM C496/C496M-17. Standard test method for splitting tensile strength of cylindrical concrete specimens*. ASTM International West Conshohocken, USA, pp. 3-5.

ASTM (2014). *ASTM C1170/C1170M-14. Standard test method for determining consistency and density of roller-compacted concrete using a vibrating table*. ASTM International West Conshohocken, USA, pp. 5-8.

ASTM (2016). *ASTM C39/C39M-16. Standard test method for compressive strength of cylindrical concrete specimens*. ASTM International West Conshohocken, USA, pp. 11-15.

British Standard Institution BSI (2011) 'BS EN 197-1:2011 Cement Part 1: Composition, specifications and conformity criteria for common cements', *BSI Standards Publication*, London, pp. 15–17.

Chaussadent, T., Baroghel-Bouny, V., Hornain, H., Rafai, N., and Ammouche, A. (2000). Effect of water-cement ratio of cement pastes on microstructural characteristics related to carbonation process. In: *Fifth CANMET/ACI International Conference on Durability of Concrete*, June 4–9, 2000, Barcelona, Spain.

Choi, Y. and Yuan, R. L. (2005). Experimental relationship between splitting tensile strength and compressive strength of GFRC and PFRC. *Cement and Concrete Research*, Vol. 35, Issue 8, pp. 1587–1591. DOI: 10.1016/j.cemconres.2004.09.010.

Dai, S. and Finkelman, R. B. (2018). Coal as a promising source of critical elements: Progress and future prospects. *International Journal of Coal Geology*, Vol. 186, pp. 155–164. DOI: 10.1016/j.coal.2017.06.005.

Emery, J. J., Guo, P., Stolle, D. F. E., Hernandez, J., and Zhang, L. (2014). Light-coloured grey asphalt pavements: from theory to practice. *International Journal of Pavement Engineering*, Vol. 15, Issue 1, pp. 23–35. DOI: 10.1080/10298436.2013.782402.

Gaedicke, C., Torres, A., Huynh, K. C. T., and Marines, A. (2016). A method to correlate splitting tensile strength and compressive strength of pervious concrete cylinders and cores. *Construction and Building Materials*, Vol. 125, pp. 271–278. DOI: 10.1016/j.conbuildmat.2016.08.031.

Haido, J. H., Tayeh, B. A., Majeed, S. S., and Karpuzcu, M. (2021). Effect of high temperature on the mechanical properties of basalt fibre self-compacting concrete as an overlay material. *Construction and Building Materials*, Vol. 268, 121725. DOI: 10.1016/j.conbuildmat.2020.121725.

Hesami, S., Modarres, A., Soltaninejad, M., and Madani, H. (2016). Mechanical properties of roller compacted concrete pavement containing coal waste and limestone powder as partial replacements of cement. *Construction and Building Materials*, Vol. 111, pp. 625–636. DOI: 10.1016/j.conbuildmat.2016.02.116.

Kaloush, K. E., Carlson, J. D., Golden, J. S., and Phelan, P. E. (2008). *The thermal and radiative characteristics of concrete pavements in mitigating urban heat island effects*. Skokie: Portland Cement Association, 139 p.

Kirthika, S. K. and Singh, S. K. (2018). Experimental investigations on basalt fibre-reinforced concrete. *Journal of The Institution of Engineers (India): Series A*, Vol. 99, Issue 4, pp. 661–670. DOI: 10.1007/s40030-018-0325-4.

LaHucik, J., Dahal, S., Roesler, J., and Amirkhanian, A. N. (2017). Mechanical properties of roller-compacted concrete with macro-fibers. *Construction and Building Materials*, Vol. 135, pp. 440–446. DOI: 1016/j.conbuildmat.2016.12.212.

Lam, M. N.-T., Jaritngam, S., and Le, D.-H. (2017). Roller-compacted concrete pavement made of Electric Arc Furnace slag aggregate: Mix design and mechanical properties. *Construction and Building Materials*, Vol. 154, pp. 482–495. DOI: 10.1016/j.conbuildmat.2017.07.240.

Levinson, R. and Akbari, H. (2002). Effects of composition and exposure on the solar reflectance of portland cement concrete. *Cement and Concrete Research*, Vol. 32, Issue 11, pp. 1679–1698. DOI: 10.1016/S0008-8846(02)00835-9.

Liang, N., Ren, L., Tian, S., Liu, X., Zhong, Z., Deng, Z., and Yan, R. (2021). Study on the fracture toughness of polypropylene–basalt fiber-reinforced concrete. *International Journal of Concrete Structures and Materials*, Vol. 15, 35. DOI: 10.1186/s40069-021-00472-x.

Masi, C. A., Schumacher, T. A., Hilman, J., Dulal, R., Rimal, G., Xu, B., Leonard, B., Tang, J., Fan, M., and Chien, T. Y. (2021). Converting raw coal powder into polycrystalline nano-graphite by metal-assisted microwave treatment. *Nano-Structures and Nano-Objects*, Vol. 25, 100660. DOI: 10.1016/j.nanoso.2020.100660.

Meddah, A., Beddar, M., and Bali, A. (2014). Use of shredded rubber tire aggregates for roller compacted concrete pavement. *Journal of Cleaner Production*, Vol. 72, pp. 187–192. DOI: 10.1016/j.jclepro.2014.02.052.

Meesaraganda, P. L. V., Dhar, D., and Rama Prasad Reddy, L. (2023). A study on basalt fiber reinforced concrete utilising seashells as replacement to coarse aggregate. *Materials Today: Proceedings*, in press. DOI: 10.1016/j.matpr.2023.03.033.

Modarres, A., Hesami, S., Soltaninejad, M., and Madani, H. (2018). Application of coal waste in sustainable roller compacted concrete pavement-environmental and technical assessment. *International Journal of Pavement Engineering*, Vol. 19, Issue 8, pp. 748–761. DOI: 10.1080/10298436.2016.1205747.

Modarres, A. and Hosseini, Z. (2014). Mechanical properties of roller compacted concrete containing rice husk ash with original and recycled asphalt pavement material. *Materials & Design*, Vol. 64, pp. 227–236. DOI: 10.1016/j.matdes.2014.07.072.

Mohammed, B. S. and Adamu, M. (2018). Mechanical performance of roller compacted concrete pavement containing crumb rubber and nano silica. *Construction and Building Materials*, Vol. 159, pp. 234–251. DOI: 10.1016/j.conbuildmat.2017.10.098.

Morgan, D. R. (1991), Freeze thaw durability of steel and polypropylene reinforced shotcretes: A review. In: *Durability of Concrete. Second International Conference.* August 4–9, 1991, Montreal, Canada.

Qin, Y., Zhao, Y., Chen, X., Wang, L., Li, F., and Bao, T. (2019). Moist curing increases the solar reflectance of concrete. *Construction and Building Materials*, Vol. 215, pp. 114–118. DOI: 10.1016/j.conbuildmat.2019.04.164.

Radović, A., Marinković, S.m and Savić, A. (2021). Compressive strength of green concrete with low cement and high filler content. *Gradjevinski materijali i konstrukcije*, Vol. 64, No. 2, pp. 93–108. DOI: 10.5937/grmk2102093r.

Ren, L.-F., Li, Q.-W., Xiao, Y., Hao, J.-C., Yi, X., Zou, L., and Li, Z.-B. (2022). Critical parameters and risk evaluation index for spontaneous combustion of coal powder in high-temperature environment. *Case Studies in Thermal Engineering*, Vol. 38, 102331. DOI: 10.1016/j.csite.2022.102331.

Reza, F. and Boriboonsomsin, K. (2015). Pavements made of concrete with high solar reflectance. In: Pacheco-Torgal, F., Labrincha, J. A., Cabeza, L. F., and Granqvist, C.-G. (eds.). *Eco-efficient Materials for Mitigating Building Cooling Needs: Design, Properties and Applications*. Woodhead Publishing, USA, pp. 37–62. DOI: 10.1016/B978-1-78242-380-5.00003-0.

Singh, N., Shehnazdeep, and Bhardwaj, A. (2020). Reviewing the role of coal bottom ash as an alternative of cement. *Construction and Building Materials*, Vol. 233, 117276. DOI: 10.1016/j.conbuildmat.2019.117276.

Vinotha Jenifer, J., Brindha, D., Annie Sweetlin Jebarani, J. P., Venkadapriya, S., and Pandieswari, M. (2023). Mechanical and microstructure properties of copper slag based basalt fiber reinforced concrete. *Materials Today: Proceedings*, in press. DOI: 10.1016/j.matpr.2023.03.505.

Xu, H., Ni, X., Su, X., Xiao, B., Luo, Y., Zhang, F., Weng, C., and Zheng, Q. (2022). Experimental investigation on the application of the coal powder as fuel in a rotating detonation combustor. *Applied Thermal Engineering*, Vol. 213, 118642. DOI: 10.1016/j.applthermaleng.2022.118642.

Yuan, Y., Zhao, R., Li, R., Wang, Y., Cheng, Z., Li, F., and Ma, Z. J. (2020). Frost resistance of fiber-reinforced blended slag and Class F fly ash-based geopolymer concrete under the coupling effect of freeze-thaw cycling and axial compressive loading. *Construction and Building Materials*, Vol. 250, 118831. DOI: 10.1016/j.conbuildmat.2020.118831.

# ОЦЕНКА БАЗАЛЬТО-ВОЛОКОННОГО АРМИРОВАННОГО УПЛОТНЕННОГО КАТКОМ БЕТОНА С ДОБАВЛЕНИЕМ УГОЛЬНОЙ ПЫЛИ ДЛЯ ДОРОЖНЫХ ПОКРЫТИЙ

Садик Альпер Йылдизель*, Кемаль Армаган

Университет Караманоглу Мехметбей, инженерный факультет, Караман, Турция

*E-mail: sayildizel@kmu.edu.tr

**Аннотация**
**Введение**: Использование цветного уплотненного катком бетона (УКБ) для дорожных покрытий с целью смягчения эффекта городского острова тепла является популярным подходом: увеличение отражения солнечной энергии может уменьшить эффект. В статье исследуется возможность применения обратного механизма для регионов с холодным климатом. Целью исследования была оценка механических и прочностных свойств, а также свойств отражения солнечной энергии УКБ с добавлением угольной пыли (УП) и базальтового волокна (БВ) для дорожных покрытий. **Методы:** для измерения альбедо использовался спектрофотометр UV-Vis-NIR. Консистенцию образцов определяли на консистометре Вебе. Прочность на сжатие, изгиб и раскалывание регистрировали через 7, 28 и 90 дней. Также была исследована морозостойкость образцов. **Результат:** Сочетание 5% УП и 0,5% БВ показало отличные характеристики для бетонных дорожных покрытий, уплотненных катком. Кроме того, полученные значения альбедо также могут повысить температуру окружающей среды в холодном климате.

**Ключевые слова:** угольная пыль, базальтовое волокно, альбедо, бетон, уплотненный катком бетон.